A novel electrospun, hydrophobic, and elastomeric styrene-butadiene-styrene membrane for membrane distillation applications

Revised Manuscript Submitted to

Journal of Membrane Science

November 2017

Hung Cong Duong[1], Dan Chuai[2], Yun Chul Woo[3], Ho Kyong Shon[3], Long Duc Nghiem[1]*, and Vitor Sencadas[2,4]*

[1] Strategic Water Infrastructure Laboratory, School of Civil, Mining and Environmental Engineering, University of Wollongong, Wollongong, NSW 2522, Australia

[2] School of Mechanical, Materials and Mechatronics Engineering, University of Wollongong, Wollongong, NSW 2522, Australia

[3] Centre for Technology in Water and Wastewater, School of Civil and Environmental Engineering, University of Technology Sydney (UTS), P.O. Box 123, 15 Broadway, NSW 2007, Australia

[4] ARC Center of Excellence for Electromaterials Science, University of Wollongong, Wollongong, NSW 2522, Australia

* Corresponding author: Long D. Nghiem, email: longn@uow.edu.au; Tel: +61 2 4221 4590
Vitor Sencadas, email: victors@uow.edu.au; Tel: +61 2 4221 4614

Abstract: In this study, a novel hydrophobic, microporous membrane was fabricated from styrene-butadiene-styrene (SBS) polymer using electrospinning and evaluated for membrane distillation applications. Compared to a commercially available polytetrafluoroethylene (PTFE) membrane, the SBS membrane had larger membrane pore size and fiber diameter and comparable membrane porosity. The fabricated SBS showed slightly lower water flux than the PTFE membrane because it was two times thicker. However, the SBS membrane had better salt rejection and most importantly could be fabricated via a simple process. The SBS membrane was also more hydrophobic than the reference PTFE membrane. In particular, as temperature of the reference water liquid increased to 60 °C, the SBS membrane remained hydrophobic with a contact angle of 100° whereas the PTFE became hydrophilic with a contact angle of less than 90°. The hydrophobic membrane surface prevented the intrusion of liquid into the membrane pores, thus improving the salt rejection of the SBS membrane. In addition, the SBS membrane had superior mechanical strength over the PTFE membrane. Using the SBS membrane, stable water flux was achieved throughout an extended MD operation period of 120 hours to produce excellent quality distillate (over 99.7% salt rejection) from seawater.

Keywords: *membrane distillation (MD); styrene-butadiene-styrene (SBS); membrane fabrication; electrospinning; seawater desalination.*

1. Introduction

Seawater desalination is an effective approach to address fresh water scarcities in many coastal cities around the world [1]. Recent technological progress in membrane technology has allowed for cost-effective seawater desalination even for municipal potable water supply. Indeed, there has been a significant increase in membrane based (especially reverse osmosis (RO)) seawater desalination plants in recent years [2]. In 2016, an estimated US $21 billion was invested on RO seawater desalination plants and this figure is expected to be doubled by 2020 [2]. However, the carbon footprint of seawater desalination is still high. Thus, there have also been many dedicated attempts to develop new membrane desalination technologies such as membrane distillation (MD) that can be readily coupled with renewable solar and geothermal energy [3].

MD is an emerging process with significant potential for seawater desalination applications [4-10]. The MD process combines thermal distillation and membrane separation. In MD, the hot saline water feed is in contact with a hydrophobic and microporous membrane. The hydrophobic nature of the membrane prevents liquid water from penetrating into the membrane pores while allowing for the permeation of water vapour. The difference in temperature across the membrane induces a water vapour pressure gradient from the feed to the distillate side, thus allowing for water vapour transport through the membrane pores. Since only water vapour can be transported across the membrane, in theory MD can offer complete salt rejection [11, 12]. In addition, unlike pressure-driven membrane processes (i.e. RO), MD operation does not require a high hydrostatic pressure. As a result, inexpensive non-corrosive materials such as plastics can be used for MD system construction. Finally, because heat is the primary energy input into the MD process, the energy costs of seawater MD desalination can be greatly reduced when low-grade heat sources such as waste heat or thermal energy can be tapped on [13-15]. Given these attributes, MD has emerged as an ideal technology platform for small-scale, off-grid, and low-cost seawater desalination processes [16-18].

Commercial realisation of seawater MD desalination has been constrained in part by the lack of suitable membrane materials [7, 19]. Given the many essential attributes of the MD membrane such as high hydrophobicity, uniform porosity, and low thermal conductivity, to date, only a few hydrophobic polymers have been used to fabricate MD membranes [20, 21]. The fabrication of most current MD membranes is a complex process involving many toxic chemicals (e.g. solvents and volatile lubricating agents) [7, 19]. In addition, current MD membrane materials such as polytetrafluoroethylene (PTFE) and polyvinylidene difluoride (PVDF) are not biodegradable. Thus, their disposal at the end of the membrane lifetime is a significant environmental issue.

There is a growing interest in new MD membrane materials to overcome the above-mentioned limitations. One of such novel materials is styrene-butadiene-styrene (SBS). SBS is a hydrophobic, thermoplastic elastomer with low thermal conductivity (i.e. 180 mW/m.K compared to 259 mW/m.K of PTFE) and excellent mechanical strength for membrane applications [22-24]. The cost of SBS is significantly lower than that of PVDF and particularly PTFE that are currently used for MD membrane fabrication. In addition, SBS is readily degradable and thus the disposal issue at the end of the membrane lifetime can be negated. Indeed, pervaporation membranes have been successfully fabricated from SBS via a simple solvent evaporation technique [22]. Several previous studies have demonstrated successful applications of these pervaporation SBS membranes for ethanol enrichment [22] and the removal of volatile organic compounds from wastewater [25]. In this work, we report an electrospinning approach to fabricate SBS membrane for MD applications. Unlike conventional membrane fabrication methods such as sintering and melt-extrusion methods, electrospinning involves only a few simple processes that can be effectively tailored to obtain membranes with desirable features for MD applications [26-28]. Electrospinning is also a versatile technique that is compatible with a range of polymeric materials and solvents [26].

The fabricated electrospun SBS membrane and a commercial MD membrane made from PTFE were evaluated and compared. Firstly, the key properties (e.g. surface morphology, wettability, and mechanical strength) of the fabricated SBS and commercial PTFE membranes were characterised and compared. Then, water flux and mass transfer coefficient of these membranes during the MD process with deionised (DI) water feed were assessed. Additionally, the desalination performance parameters including water flux and salt rejection of the fabricated SBS membrane was compared to those of the commercial PTFE membrane during the MD process with a synthetic saline feed. Finally, the feasibility of the electrospun SBS membrane for seawater desalination was demonstrated during a long term MD experiment process using seawater as the feed.

2. Materials and methods

2.1. Preparation of the electrospun SBS membrane

The SBS membrane was prepared from a polymer solution with the SBS concentration of 15 wt.% using the electrospinning method. Linear tri-block SBS copolymer (C540 Calprene, Dyansol) was dissolved in a mixture of analytical grade tetrahydrofuran (THF, Sigma Aldrich) and dimethylformamide (DMF, Sigma Aldrich) (i.e. with a volumetric ratio of 75/25) at room

temperature with the help of a magnetic stirrer (MST, VELP). The SBS solution was then transferred to a commercial Luer-Lock syringe, fitted with a 22-Gauge metallic needle prior to the electrospinning processing. The electrospinning process was conducted under an electric field of 1.0 kV/cm generated by a high voltage source (Gamma High Voltage Research Inc.). During the electrospinning process, a syringe pump (KDScientific) was used to continually feed the polymer solution into the needle tip. Electrospun fibers were collected on a grounded metallic plate, and at temperature and relative humidity of 21 ± 2 °C and 43 ± 5%, respectively. Subsequent to the electrospinning process, the fabricated membranes were stored at temperature of 40 ± 1 °C and low pressure of 93 kPa in a temperature-controlled vacuum chamber (Shel Lab, Model 1410D) for at least 48 hours to completely remove any remaining solvent.

A commercially available PTFE (Porous Membrane Technology, Ningbo, China) was used to bench-mark our novel SBS membrane. Detailed characteristics of this PTFE membrane are available elsewhere [29].

2.2. Membrane characterisation

2.2.1. Membrane surface morphology

Morphology of the SBS and PTFE membranes was characterised using a low vacuum scanning electron microscopy (SEM) (i.e. JSM-6490LV provided by JOEL, Japan) and atomic force microscopy (AFM). Prior to SEM analysis, the membrane samples were coated with a thin layer of gold using a sputter coater (Smart Coater, JEOL). Subsequent to SEM analysis, the fiber diameters and their distribution of the two membranes were determined using ImageJ software [30]. AFM imaging was conducted in non-contact mode and under room conditions using silicon probes (Dimension 3100 Scanning Probe Microscope, Bruker) to evaluate surface roughness of the membrane samples. Three membrane locations (10×10 μm^2) were randomly selected for scanning. The average membrane mean surface roughness (R_a) was then calculated using the NanoScope Analysis software.

2.2.2. Membrane porosity, pore size, and pore size distribution

The porosity (ε) of the membrane samples was obtained using the pycnometer method [26, 31], and was calculated as:

$$\varepsilon = \frac{\left(W_2 - W_3 - W_s\right)}{W_1 - W_3} \quad (1)$$

where W_1, W_2, W_3, and W_s were the weight of the pycnometer filled with absolute alcohol, the pycnometer filled with absolute alcohol and the immersed sample, the pycnometer without the saturated sample, and the dry membrane sample, respectively.

A capillary flow porometry (Porolux 1000) was used to determine the pore size and pore size distribution of the fabricated electrospun SBS and commercial PTFE membrane samples. Detailed description of the method used is provided elsewhere [32].

2.2.3. Membrane surface hydrophobicity and liquid entry pressure

The surface hydrophobicity of the membranes was evaluated using water-membrane contact angle measurements. The contact angle of the membranes was measured by the sessile drop method using a Rame-Hart Goniometer (Model 250, Rame-Hart, Netcong, New Jersey, USA) with deionised (DI) water as a reference. DI water droplets (12 μL) were deposited on the membrane and the contact angles between the droplets and the membrane surface were determined. A temperature-controlled chamber (Model P/N 100-07) was integrated with the Rame-Hart Goniometer to facilitate the measurements of contact angle at different temperatures (e.g. 25, 50, 55, and 60 °C). After placing the membrane inside the chamber, the temperature of the chamber was increased to a desired value and stabilised for 5 minutes. A drop of water was then placed on top of the membrane and the contact angle was recorded within 60 seconds. At least 5 droplets were deposited at different locations of each membrane sample for contact angle measurement.

Liquid entry pressure (*LEP*) of the membrane was determined using a custom-made apparatus (Supplementary Data, **Fig. S1**). The *LEP* apparatus consisted of a cylindrical cell connected with a nitrogen gas bottle [33]. The cylindrical cell had a movable silicon base. DI water was filled into the cell, then a dry membrane sample (i.e. effective surface area of 7 cm^2) was secured to the cell on the top of water to form a chamber. The pressure caused by nitrogen gas at the bottom of the water-filled chamber pushed the silicone base and water against the membrane. The nitrogen gas pressure was increased stepwise. The applied pressure at which the first water bubble appeared on the top membrane surface was recorded as the *LEP* value of the membrane. Triplicate measurements were conducted for each membrane sample.

2.2.4. Membrane mechanical strength

Stress-strain measurements were performed to assess the mechanical strength of the fabricated SBS and commercial PTFE membranes. The measurements were conducted at 25 °C using a Shimadzu Universal Testing Machine (EZ-SX) with a 10 N load cell in tensile mode, and

at a strain rate of 1 mm/min. Rectangular stripes (i.e. with a size of 10 × 40 mm^2) were measured with a caliper (Mitutoyo) and a thickness (SBS = 200 µm and PTFE = 300 µm) was measured with a DUALSCOPE® MPOR (Fischer). From the stress-strain data, elastic modulus was calculated in the linear zone, between 0 and 2% of strain, for all the samples. The ultimate tensile strength and the strain-at-failure were also determined. The stress-strain measurements were performed using five different specimens.

2.3. Membrane distillation performance evaluation

A lab-scale direct contact MD system (**Fig. 1**) was used to assess the distillation performance (e.g. water flux, mass transfer coefficient, and salt rejection) of the fabricated SBS and the commercial PTFE membranes for comparison purposes. The test system consisted of a plate-and-frame MD membrane module and hot feed and cold distillate cycles. The membrane module composed of two acrylic semi-cells; each cell was engraved to create a flow channel with depth, width, and length of 0.3, 4.5, and 9.0 cm, respectively. A membrane coupon was sandwiched between the two semi-cells to form the feed and distillate channels.

Feed water in the MD feed tank was heated using a submerged heating element connected to a temperature control unit. A chiller with heat-exchanging coils submerged directly into the distillate tank was used to control the distillate temperature. Two variable-speed gear pumps (Model 120/IEC71-B14, Micropump Inc.) were used to circulate the feed and distillate through the membrane module. A digital balance (PB32002-S, Mettler Toledo, Inc.) connected to a computer was used to weigh the mass of the feed tank and determine the water flux.

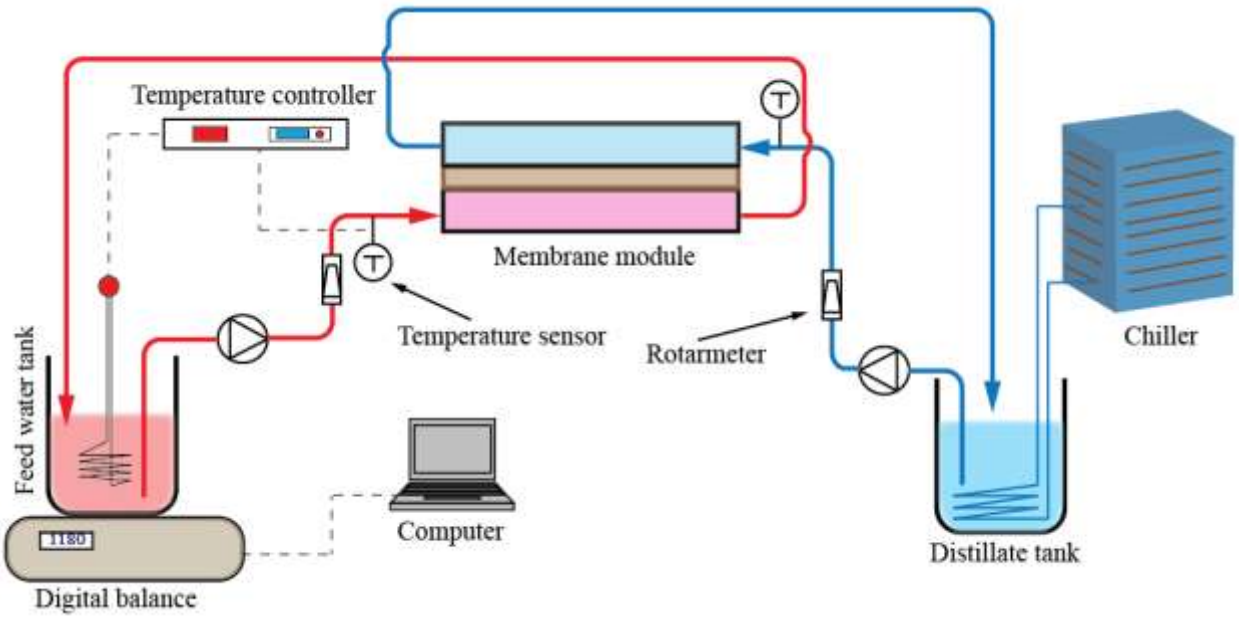

Fig. 1. The schematic diagram of the MD test unit.

DI water, synthetic NaCl solution, and pre-filtered seawater were used as feed solutions. DI water (i.e. with electrical conductivity of 40 μS/cm) was obtained from a Milli-Q water purification system (Millipore). Analytical grade NaCl was dissolved in DI water to prepare the synthetic solution. Seawater from Wollongong beach (New South Wales, Australia) was pre-filtered by 0.5 μm filter papers. The pre-filtered seawater had conductivity, pH, and total dissolved solids of 51.5 mS/cm, 8.32, and 35 g/L, respectively. The total organic carbon (TOC) concentration of this pre-filtered seawater was negligible (<2 mg/L) [34].

The MD process with DI water was conducted to evaluate the water transfer through the membranes. DI water feed at temperatures of 50, 55, and 60 °C was circulated through the feed channel at a rate of 0.5 L/min (i.e. equivalent to cross-flow velocity of 0.06 m/s). DI water (4 L) was used as initial distillate, and was circulated through the distillate channel at the same rate to the feed. The distillate temperature was maintained constant at 20 °C. Water flux of the process at each feed temperature was recorded for two hours after the attainment of stable conditions. The mass transfer coefficient (K_m) of the MD system was determined following the method described by Duong et al. [35].

The MD process with synthetic NaCl solution and pre-filtered seawater feeds was experimented to test the desalination efficiency (e.g. water flux and salt rejection) of the membranes. The operating conditions were similar to those described above. During the experiments, the obtained distillate was returned to the feed tank to maintain a constant feed salinity. The electrical conductivity of the feed and distillate was measured with a conductivity meter (Orion Star A322, ThermoFisher). The salt rejection ($S_{rejection}$) of the membranes was calculated using Eq. 2 given the negligible salt concentration of the initial distillate [16, 36]:

$$S_{rejection} = \left(1 - \frac{EC_{distillate}}{EC_{feed}}\right) \times 100\% \quad (2)$$

where $EC_{distillate}$ and EC_{feed} were electrical conductivity of the distillate and the feed, respectively. For the MD experiments with the synthetic NaCl solution feed, the feed and distillate conductivities were measured 2 hours after the water flux has been stabilised.

3. Results and discussions

3.1. Membrane characterisation

3.1.1. Membrane morphology

SEM images confirmed that the fabricated SBS membrane exhibited a microporous structure similar to that of the PTFE membrane (**Fig. 2**). Both the SBS and PTFE membrane had micro pores formed by interconnected fibers on their surfaces. The SBS membrane had a mean pore size of 0.58 µm whereas that of the PTFE membrane was 0.46 µm. However, the SBS membrane was composed of larger fibers (**Fig. 2**); thus, it exhibited a slightly lower porosity compared to the PTFE membrane (i.e. 81% compared to 85%).

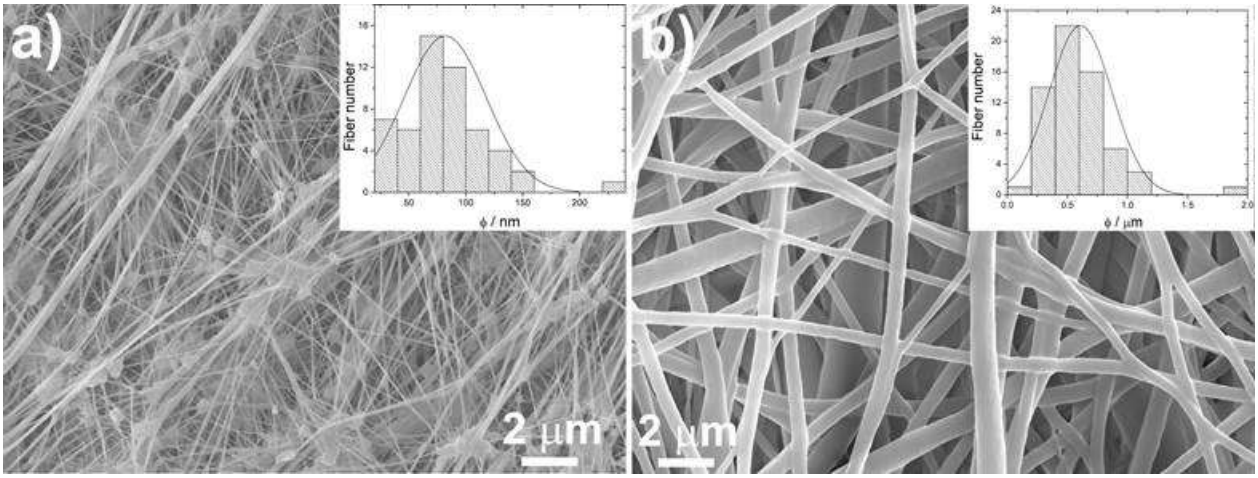

Fig. 2. Morphology of (a) the commercial PTFE membrane and (b) the fabricated SBS membrane. The insets present the fiber diameters distribution of the membrane samples.

The difference in fiber diameters and pore sizes led to a notable difference in the surface roughness between the fabricated SBS and commercial PTFE membranes. The SBS membrane exhibited a surface roughness of 457.4 ± 36.5 nm, considerably rougher than PTFE membrane surface (surface roughness of 235.4 ± 38.2 nm). Consistent with the SEM images, while the AFM image of the PTFE membrane revealed randomly aligned fibers with small diameters, the SBS membrane surface was composed of significantly larger fibers (Supplementary Data, **Fig. S2**). Large fibers together with large voids between individual fibers rendered the higher surface roughness of the SBS membrane compared to that of the PTFE one.

SEM micrographs of the membrane cross section showed the SBS membrane thickness of 200 µm, which is four times thicker than the active layer of the PTFE membrane. A thicker membrane exhibits lower water flux but higher thermal efficiency due to a reduced heat loss via

conduction through the membrane [4, 6]. The comparison in water flux of the MD process with the SBS and the PTFE membrane is discussed in the section 3.2.

3.1.2. Membrane wettability

The wettability of the membrane during the MD process depends on membrane properties (e.g. surface hydrophobicity and membrane pore size) and operating conditions. The membrane wettability can be assessed using water-membrane contact angle and liquid entry pressure (*LEP*). The contact angle measurements demonstrated the superior surface hydrophobicity of the fabricated SBS over the commercial PTFE membrane. At room temperature, while the PTFE membrane exhibited a contact angle of 117 ± 2°, that value of the fabricated SBS was 132 ± 2° (**Fig. 3**). Increasing temperature led to a decline in the contact angles of both PTFE and SBS membranes. It is, however, noteworthy that as the temperature reached 60 °C, while the SBS membrane surface remained hydrophobic with a contact angle of 100°, the hydrophobicity of the PTFE membrane had been significantly deteriorated (i.e. with contact angle < 90°) (**Fig. 3**). The decline in the membrane surface hydrophobicity with increased temperature can be attributed to the decreased water surface tension [37, 38] and changes in the membrane morphology [38].

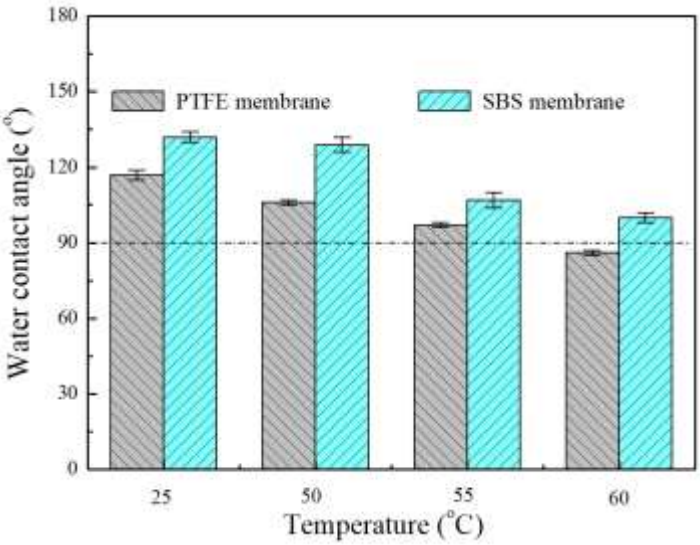

Fig. 3. Water contact angle of the commercial PTFE and the fabricated SBS membranes at various temperatures. DI water was used as the reference liquid. Error bars represent standard deviations of 50 measurements.

The SBS membrane had a lower *LEP* as compared with the commercial PTFE membrane despite a higher surface hydrophobicity as discussed above. The *LEP* of the SBS membrane was less than a half of that of the PFFE membrane (i.e. 81.0 ± 0.6 kPa compared to 192.0 ± 0.9 kPa). The difference between the *LEP* of the fabricated SBS and commercial PTFE membranes can be

attributed to the difference in their pore size and pore structure. *LEP* depends on membrane pore size and structure and membrane surface hydrophobicity as expressed in Eq. 3:

$$LEP = \frac{-2B\gamma_l \cos\theta}{r_{\max}} \quad (3)$$

where B is a factor representing the geometry of the pores, γ_l is liquid surface tension, θ is the contact angle of the membrane, and r_{max} is the maximum membrane pore size. The fabricated SBS membrane had a higher contact angle, but its maximum pore size was much larger (i.e. 1.55 µm compared to 1.12 µm); thus, it demonstrated a lower *LEP* compared to the PTFE membrane. It is worth noting that the fabricated SBS membrane is compatible with MD applications with respects to membrane wetting resistance. Indeed, the *LEP* value of most commercially available flat-sheet MD membranes varies in a wide range from 48 to 463 kPa, depending on membrane material and fabrication methods used [39].

3.1.3. Membrane mechanical strength

The stress-strain measurement results demonstrated higher mechanical strength of the SBS membrane compared to the PTFE membrane (**Fig. 4**). The SBS samples underwent yielding, necking and strain hardening when the strain was increased. During the initial mechanical loading, the SBS fibers started rotating and aligning in the direction of the applied stress, followed by a necking formation. At higher strain, an increase of the fiber alignment in the direction of the mechanical load, which led to an increase of the stress recorded and was followed by void growth, induced softening. As a result, the SBS membrane exhibited a maximum stress and strain of 525 ± 50 kPa and 345 ± 30%, respectively, and an elastic modulus of 9.8 ± 0.7 MPa. On the other hand, the commercial PTFE membrane was more brittle with maximum stress and strain of 3300 ± 230 kPa and 101 ± 15%, respectively, and an elastic modulus of 37.2 ± 6.1 MPa (**Fig. 4**).

It is noted that the mechanical strength of the fabricated membranes is lower than that reported for bulk SBS material [40]. This can be attributed to the considerably lower density (higher porosity) of the membrane samples as compared to bulk SBS material. Furthermore, in the SBS membrane samples, the fibers are arranged in a nonwoven fashion and only a portion of them contribute to the resistance to the applied mechanical loading, hence resulting in fewer chain entanglements per unit of mass of the porous membrane as compared to the bulk SBS material.

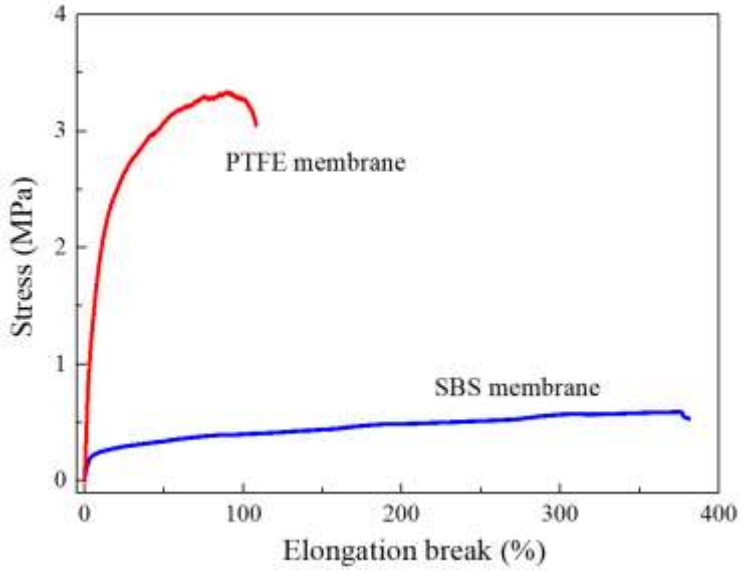

Fig. 4. Stress-strain curves of the fabricated SBS and commercial PTFE membranes.

3.2. MD performance

3.2.1. Water flux

The MD process with the SBS membrane achieved lower water flux than that with the commercial PTFE membrane when DI water was used as the feed (**Fig. 5a**). The lower water flux of the SBS membrane was mostly due to its higher thickness as compared to the commercial PTFE membrane. Indeed, the thickness of the SBS membrane was two times of that of the PTFE membrane. It is well-established that water flux of the MD process is inversely proportional to the membrane thickness due to increased membrane resistance to the transfer of water vapour [4, 6]. Lower porosity of the SBS membrane is also a factor limiting its water flux when comparing to the PTFE membrane.

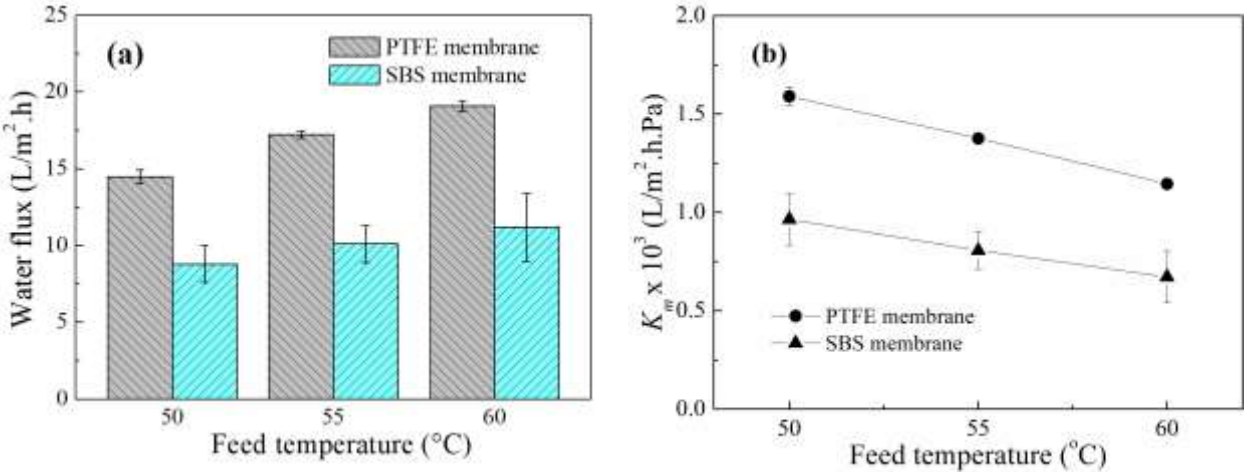

Fig. 5. (a) Water flux and (b) mass transfer coefficient (K_m) as functions of operating feed temperature during the MD process using the PTFE membrane and the fabricated SBS membrane with the DI water feed. Operating conditions: feed and distillate circulation rates of 0.5 L/min (i.e. cross flow velocities of 0.06 m/s), distillate temperature of 20 °C. The error bars represent the standard deviation of five measurements.

The analysis of the process mass transfer coefficient (K_m) demonstrated a less severe temperature polarisation effect of the MD process with the SBS membrane compared to that with the PTFE membrane. The determination of K_m involved the temperatures in the bulk feed and distillate streams instead of at the membrane surfaces; therefore, temperature polarisation effect was embedded in K_m [35, 41]. Elevating feed temperature increases water flux and hence exacerbates the temperature polarisation effect [42, 43]. As a result, the K_m values of the process with both SBS and PTFE membranes decreased when the feed temperature increased (**Fig. 5b**). However, K_m of the process with the SBS membrane decreased at a slightly lower rate than that of the process with the PTFE membrane (**Fig. 5b**).

3.2.2. Desalination performance

Desalination efficiency (i.e. water flux and salt rejection) of the two membranes was compared during the MD process with NaCl solutions. Given its lower K_m, water flux of the MD process using the SBS membrane was lower than that of the process with the PTFE membrane under the same operating condition (e.g. feed salinity, feed and distillate temperatures). In addition, the process water flux from both the SBS and PTFE membranes decreased when the feed salinity increased from 1 to 105 g/L as NaCl. This observed decrease in the process water flux can be attributed to two factors: decreased feed water activity (i.e. colligative property of the feed) and polarisation effects.

Increasing feed salinity reduces the feed water activity, and hence results in a lower water vapour pressure of the feed stream, thus reducing the process water flux [4, 7]. For a dilute solution, the effect of feed water activity on water vapour pressure can be estimated as [6]:

$$P = x_{water}(1 - 0.5 \times x_{salt} - 10 \times {x_{salt}}^2)P_o \quad (4)$$

where P_o is the water vapour pressure of pure water; x_{water} and x_{salt} are the molar fraction of water and salts, respectively. Based on Eq. (4), as the feed salinity increases from 1 to 105 g/L, the water vapour pressure decreases by only 3%. Thus, polarisation appears to play a much more significant role in this study.

The concentration polarisation effect was expected to be negligible when 1 g/L NaCl solution was used as the feed. As the feed salinity increased, concentration polarisation became more

significant and temperature polarisation was also exacerbated due to the increase in feed viscosity. Therefore, water flux of the MD process decreased faster as the feed salinity increased beyond 70 g/L, especially for the commercial PTFE membrane (**Fig. 6a**). In comparison to the PTFE membrane, water flux from the SBS membrane was relatively stable when the feed salinity increased from 1 to 70 g/L (**Fig. 6a**). This is because the SBS membrane had a lower water flux and hence was less affected by concentration and temperature polarisation effects [4, 12].

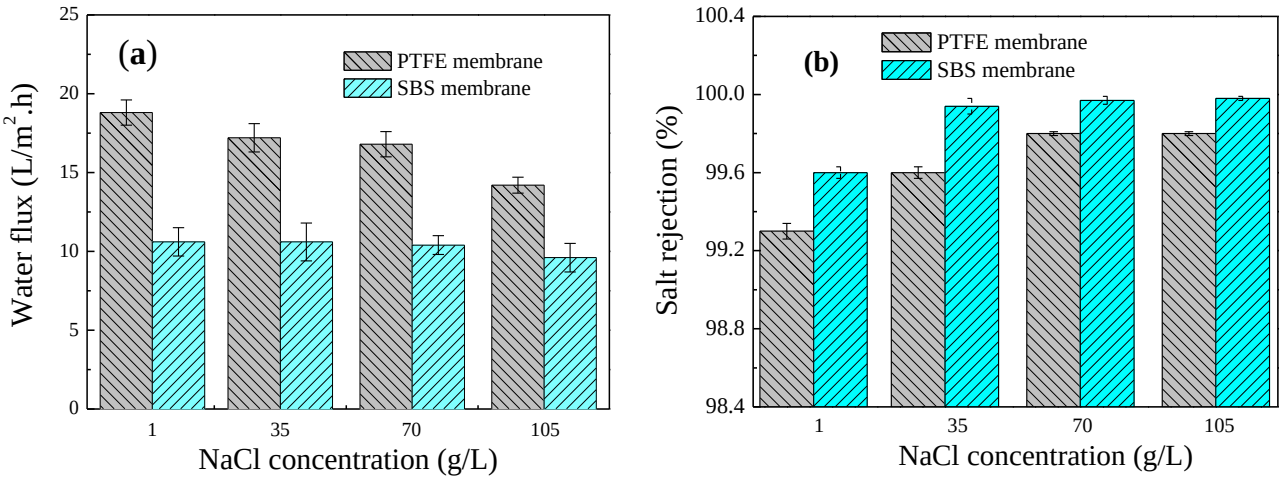

Fig. 6. Water flux and salt rejection of the fabricated SBS and PTFE membranes during the MD process with the synthetic NaCl solution feed at different feed salinity. Other operating conditions: feed temperature of 60 °C, distillate temperature of 20 °C, feed and distillate circulation rates of 0.5 L/min (i.e. cross flow velocities of 0.06 m/s). The error bars represent the standard deviation of five measurements.

The MD process with the SBS membrane achieved a higher salt rejection than that with the PTFE membrane at all NaCl concentrations (**Fig. 6b**). This is consistent with the higher surface hydrophobicity and roughness of the SBS membrane compared to those of the PTFE membrane. Indeed, improved salt rejection associated with enhanced membrane hydrophobicity and roughness has been reported in previous studies [27, 44]. Increased membrane surface hydrophobicity and roughness result in a more efficient insulation layer between the liquid and membrane surface, thus limiting the intrusion of salt into the membrane pores [27, 44]. The superior salt rejection by the SBS membrane is particularly useful for the separation of high value minerals such as in liquid desiccant regeneration for air conditioning systems [29] or the recovery of these minerals from diluted brines [45].

Long-term performance of the SBS and commercial PTFE membranes was demonstrated using pre-filtered seawater. During the MD process with the pre-filtered seawater feed, the produced distillate was returned to the feed tank to maintain a constant feed salinity (i.e. 35 g/L).

After 120 hours of continuous operation, water flux of the MD process using SBS and PTFE membrane remained constant (**Fig. 7a**). No evidence of membrane fouling or scaling was observed at the end of the experiment.

The observed salt rejection also confirmed the absence of membrane fouling during the MD process with the pre-filtered seawater feed using the SBS and PTFE membranes. Salt rejection by both the SBS and PTFE membranes gradually increased over the first 35 hours of the operation, then stabilised at 99.97% until the end of the long-term experiment (**Fig. 7b**).

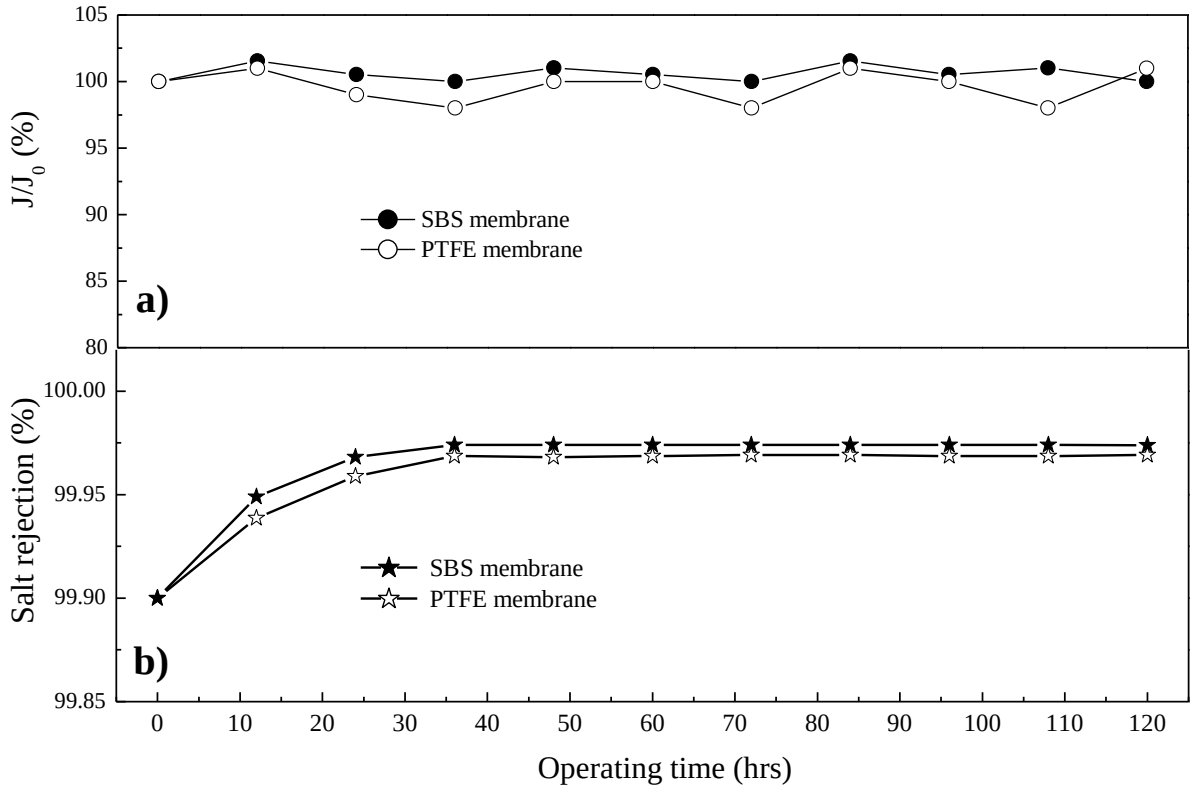

Fig. 7. Normalised water flux (J/J_0) and salt rejection during the MD process of pre-filtered seawater feed. Operating conditions: feed temperature of 60 °C, distillate temperature of 20 °C, feed and distillate circulation rates of 0.5 L/min (i.e. cross flow velocities of 0.06 m/s). The salinity of the seawater feed was maintained constant by returning the distillate back to the feed tank throughout the experiments.

3.3. Feasibility consideration

The summary of the membrane characteristics and distillation performance of the SBS and PTFE membrane is provided in **Table 1**. This new SBS membrane is superior to the commercial PTFE membrane with respect to mechanical properties and surface hydrophobicity. The SBS membrane exhibits a noticeably lower elastic modulus than the PTFE membrane given the presence of soft monomeric units in SBS. On the other hand, both membranes are comparable in

terms of porosity. The higher surface roughness and the superior surface hydrophobicity, especially at high temperatures, also induces higher salt rejection for the SBS membrane as compared to the PTFE one. Improved salt rejection and resistance to polarisation effects are possibly crucial to the MD applications for regeneration of hyper saline solutions such as liquid desiccant solution or forward osmosis draw solution. Nevertheless, further improvement is required to improve the water flux of the SBS membrane, which was considerably lower compared to the commercial PTFE membrane. The observed low water flux by the SBS membrane is attributed to its significantly higher membrane thickness (hence higher membrane mass transfer resistance). SBS is a soft elastomer; thus, a thick electrospun SBS layer is required to produce flat sheet membrane for MD operation. It is envisioned that by producing a thin film composite membrane in which a supporting layer can be used to provide the mechanical stiffness to prevent curving can potentially be used to address this issue in a future study.

Overall, the SBS membrane promises to be a strong competitor for the PTFE membrane concerning the membrane production and disposal costs. Raw SBS is biodegradable and more affordable than PTFE – the fabrication of the SBS membrane involves only a single electrospinning step and low cost raw materials, while the PTFE membrane manufacturing entails complicated multi-stage processes with costly raw materials and toxic additives. The biodegradability of the SBS membrane also helps to negate the disposal issues when MD membrane modules are disposed at the end of their lifetime.

Table 1. Comparisons between the commercial PTFE and the fabricated SBS membrane.

Sample	Porosity (%)	Thickness (μm)	Mean pore size (μm)	*Roughness* (nm)	Contact angle[a] (°)	*E*[b] (MPa)	Flux[c] (L/m^2.h)
PTFE membrane	85 ± 10	100 ± 7	0.46	235.4 ± 38.2	117 ± 2	37.2 ± 6.1	19.1 ± 0.3
SBS membrane	81 ± 4	200 ± 15	0.58	457.4 ± 36.5	132 ± 2	9.8 ± 0.7	11.2 ± 2.2

[a] with DI water at 25 °C
[b] elastic modulus
[c] with DI water feed and operated at feed and distillate temperature of 60 and 25 °C, water circulation rate of 0.5 L/min

4. Conclusions

A novel hydrophobic, microporous membrane based on styrene-butadiene-styrene (SBS) polymer was prepared using the electrospinning method. The SBS membrane was systematically evaluated in comparison to a commercial polytetrafluoroethylene (PTFE) membrane. The SBS membrane had larger membrane pore sizes and fiber diameters but comparable membrane porosity compared to the PTFE one. The fabricated SBS membrane was two times thicker, and thus had a lower water flux than the PTFE membrane. Nevertheless, the SBS membrane showed

better salt rejection, higher surface hydrophobicity and superior mechanical strength over the reference PTFE membrane. The high membrane surface hydrophobicity prevented the intrusion of liquid into the membrane pores, thus improving the salt rejection of the SBS membrane. The SBS membrane showed stable water flux and excellent salt rejection (i.e. >99.97%) throughout a long term MD operation using seawater as the feed. The results from this study reveal great potential of SBS as a promising alternative to conventional MD membrane materials for desalination applications.

References

1. M. Elimelech and W.A. Phillip, The Future of Seawater Desalination: Energy, Technology, and the Environment, Science 333 (2011) 712-717.
2. B.E. Logan, The Global Challenge of Sustainable Seawater Desalination, Environ. Sci. Technol. Lett. 4 (2017) 197-197.
3. A. Ali, R.A. Tufa, F. Macedonio, E. Curcio, and E. Drioli, Membrane technology in renewable-energy-driven desalination, Renew. Sustainable Energy Rev. 81 (2018) 1-21.
4. A. Alkhudhiri, N. Darwish, and N. Hilal, Membrane distillation: A comprehensive review, Desalination 287 (2012) 2-18.
5. D. González, J. Amigo, and F. Suárez, Membrane distillation: Perspectives for sustainable and improved desalination, Renew. Sustainable Energy Rev. 80 (2017) 238-259.
6. K.W. Lawson and D.R. Lloyd, Membrane distillation, J. Membr. Sci. 124 (1997) 1-25.
7. P. Wang and T.-S. Chung, Recent advances in membrane distillation processes: Membrane development, configuration design and application exploring, J. Membr. Sci. 474 (2015) 39-56.
8. X.M. Li, B. Zhao, Z. Wang, M. Xie, J. Song, L.D. Nghiem, T. He, C. Yang, C. Li, and G. Chen, Water reclamation from shale gas drilling flow-back fluid using a novel forward osmosis-vacuum membrane distillation hybrid system, Water Sci. Technol. 69 (2014) 1036-1044.
9. F. Suárez, J.A. Ruskowitz, S.W. Tyler, and A.E. Childress, Renewable water: Direct contact membrane distillation coupled with solar ponds, Appl. Energ. 158 (2015) 532-539.
10. S. Meng, Y.-C. Hsu, Y. Ye, and V. Chen, Submerged membrane distillation for inland desalination applications, Desalination 361 (2015) 72-80.
11. H.C. Duong, P. Cooper, B. Nelemans, T.Y. Cath, and L.D. Nghiem, Evaluating energy consumption of membrane distillation for seawater desalination using a pilot air gap system, Sep. Purif. Technol. 166 (2016) 55-62.
12. H.C. Duong, M. Duke, S. Gray, T.Y. Cath, and L.D. Nghiem, Scaling control during membrane distillation of coal seam gas reverse osmosis brine, J. Membr. Sci. 493 (2015) 673-682.

13. K. Manzoor, S.J. Khan, Y. Jamal, and M.A. Shahzad, Heat extraction and brine management from salinity gradient solar pond and membrane distillation, Chem. Eng. Res. Des. 118 (2017) 226-237.

14. N. Dow, S. Gray, J.-d. Li, J. Zhang, E. Ostarcevic, A. Liubinas, P. Atherton, G. Roeszler, A. Gibbs, and M. Duke, Pilot trial of membrane distillation driven by low grade waste heat: Membrane fouling and energy assessment, Desalination 391 (2016) 30-42.

15. N. Ghaffour, J. Bundschuh, H. Mahmoudi, and M.F.A. Goosen, Renewable energy-driven desalination technologies: A comprehensive review on challenges and potential applications of integrated systems, Desalination 356 (2015) 94-114.

16. W.G. Shim, K. He, S. Gray, and I.S. Moon, Solar energy assisted direct contact membrane distillation (DCMD) process for seawater desalination, Sep. Purif. Technol. 143 (2015) 94-104.

17. A. Chafidz, S. Al-Zahrani, M.N. Al-Otaibi, C.F. Hoong, T.F. Lai, and M. Prabu, Portable and integrated solar-driven desalination system using membrane distillation for arid remote areas in Saudi Arabia, Desalination 345 (2014) 36-49.

18. R. Schwantes, A. Cipollina, F. Gross, J. Koschikowski, D. Pfeifle, M. Rolletschek, and V. Subiela, Membrane distillation: Solar and waste heat driven demonstration plants for desalination, Desalination 323 (2013) 93-106.

19. L. Eykens, K. De Sitter, C. Dotremont, L. Pinoy, and B. Van der Bruggen, Membrane synthesis for membrane distillation: A review, Sep. Purif. Technol. 182 (2017) 36-51.

20. E. Drioli, A. Ali, and F. Macedonio, Membrane distillation: Recent developments and perspectives, Desalination 356 (2015) 56-84.

21. B.L. Pangarkar, S.K. Deshmukh, V.S. Sapkal, and R.S. Sapkal, Review of membrane distillation process for water purification, Desalin. Water Treat. 57 (2016) 2959-2981.

22. S. Santoro, F. Galiano, J.C. Jansen, and A. Figoli, Strategy for scale-up of SBS pervaporation membranes for ethanol recovery from diluted aqueous solutions, Sep. Purif. Technol. 176 (2017) 252-261.

23. J.-J. Chen, S.-H. Qin, Q.-C. Lv, D.-L. Shi, X.-M. Zheng, H.-J. Wu, H.-K. Huang, L.-G. Lian, F.-A. He, and K.-H. Lam, Preparation of novel xGNPs/SBS composites with enhanced dielectric constant and thermal conductivity, Adv. Polym. Technol. (2017) 1-8.

24. D.M. Price and M. Jarratt, Thermal conductivity of PTFE and PTFE composites, Thermochimica Acta 392-393 (2002) 231-236.

25. B.K. Dutta and S.K. Sikdar, Separation of Volatile Organic Compounds from Aqueous Solutions by Pervaporation Using SBS Block Copolymer Membranes, Environ. Sci. Technol. 33 (1999) 1709-1716.

26. L.D. Tijing, J.-S. Choi, S. Lee, S.-H. Kim, and H.K. Shon, Recent progress of membrane distillation using electrospun nanofibrous membrane, J. Membr. Sci. 453 (2014) 435-462.

27. Z. Xu, Z. Liu, P. Song, and C. Xiao, Fabrication of super-hydrophobic polypropylene hollow fiber membrane and its application in membrane distillation, Desalination 414 (2017) 10-17.

28. N.S. Abdul-Halim, P.G. Whitten, and L.D. Nghiem, Characteristics and cadmium extraction performance of PVC/Aliquat 336 electrospun fibres in comparison with polymer inclusion membranes, Sep. Sci. Technol. 51 (2016) 1515-1522.

29. H.C. Duong, F.I. Hai, A. Al-Jubainawi, Z. Ma, T. He, and L.D. Nghiem, Liquid desiccant lithium chloride regeneration by membrane distillation for air conditioning, Sep. Purif. Technol. 177 (2017) 121-128.

30. C.A. Schneider, W.S. Rasband, and K.W. Eliceiri, NIH Image to ImageJ: 25 years of image analysis, Nat Meth 9 (2012) 671-675.

31. Y. Yan, V. Sencadas, J. Zhang, D. Wei, and Z. Jiang, Superomniphilic Poly(glycerol sebacate)-Poly(l-lactic acid) Electrospun Membranes for Oil Spill Remediation, Adv. Mater. Interfaces 4 (2017) 1700484, DOI: 10.1002/admi.201700484.

32. Y.C. Woo, Y. Kim, W.-G. Shim, L.D. Tijing, M. Yao, L.D. Nghiem, J.-S. Choi, S.-H. Kim, and H.K. Shon, Graphene/PVDF flat-sheet membrane for the treatment of RO brine from coal seam gas produced water by air gap membrane distillation, J. Membr. Sci. 513 (2016) 74-84.

33. Y.C. Woo, L.D. Tijing, W.-G. Shim, J.-S. Choi, S.-H. Kim, T. He, E. Drioli, and H.K. Shon, Water desalination using graphene-enhanced electrospun nanofiber membrane via air gap membrane distillation, J. Membr. Sci. 520 (2016) 99-110.

34. H.C. Duong, M. Duke, S. Gray, P. Cooper, and L.D. Nghiem, Membrane scaling and prevention techniques during seawater desalination by air gap membrane distillation, Desalination 397 (2016) 92-100.

35. H.C. Duong, P. Cooper, B. Nelemans, and L.D. Nghiem, Optimising thermal efficiency of direct contact membrane distillation via brine recycling for small-scale seawater desalination, Desalination 374 (2015) 1-9.

36. L. Francis, N. Ghaffour, A.S. Alsaadi, S.P. Nunes, and G.L. Amy, Performance evaluation of the DCMD desalination process under bench scale and large scale module operating conditions, J. Membr. Sci. 455 (2014) 103-112.

37. M. de Ruijter, P. Kölsch, M. Voué, J. De Coninck, and J.P. Rabe, Effect of temperature on the dynamic contact angle, Colloids Surf. A Physicochem. Eng. Asp. 144 (1998) 235-243.

38. J. Ge, Y. Peng, Z. Li, P. Chen, and S. Wang, Membrane fouling and wetting in a DCMD process for RO brine concentration, Desalination 344 (2014) 97-107.

39. Gábor Rácz, Steffen Kerker, Zoltán Kovács, Gyula Vatai, Mehrdad Ebrahimi, and P. Czermak, Theoretical and Experimental Approaches of Liquid Entry Pressure Determination in Membrane Distillation Processes, Period. Polytech. Chem. Eng. 58 (2014) 81-91.

40. P. Costa, J. Silva, V. Sencadas, R. Simoes, J.C. Viana, and S. Lanceros-Méndez, Mechanical, electrical and electro-mechanical properties of thermoplastic elastomer styrene-butadiene-styrene/multiwall carbon nanotubes composites, J. Mater. Sci. 48 (2013) 1172-1179.

41. H.C. Duong, M. Duke, S. Gray, B. Nelemans, and L.D. Nghiem, Membrane distillation and membrane electrolysis of coal seam gas reverse osmosis brine for clean water extraction and NaOH production, Desalination 397 (2016) 108-115.

42. P. Termpiyakul, R. Jiraratananon, and S. Srisurichan, Heat and mass transfer characteristics of a direct contact membrane distillation process for desalination, Desalination 177 (2005) 133-141.

43. J. Phattaranawik, R. Jiraratananon, and A.G. Fane, Heat transport and membrane distillation coefficients in direct contact membrane distillation, J. Membr. Sci. 212 (2003) 177-193.

44. D. Zhao, J. Zuo, K.-J. Lu, and T.-S. Chung, Fluorographite modified PVDF membranes for seawater desalination via direct contact membrane distillation, Desalination 413 (2017) 119-126.

45. X. Ji, E. Curcio, S. Al Obaidani, G. Di Profio, E. Fontananova, and E. Drioli, Membrane distillation-crystallization of seawater reverse osmosis brines, Sep. Purif. Technol. 71 (2010) 76-82.